Applied Condition Monitoring

Ahmed Hammami ·
Philippus Stephanus Heyns ·
Stephan Schmidt · Fakher Chaari ·
Mohamed Slim Abbes ·
Mohamed Haddar *Editors*

Modelling and Simulation of Complex Systems for Sustainable Energy Efficiency

Contributions to the First International Workshop on Modelling and Simulation of Complex Systems for Sustainable Energy Efficiency, MOSCOSSEE'2021, February 25–26, 2021

Springer

Applied Condition Monitoring

Volume 20

The book series Applied Condition Monitoring publishes the latest research and developments in the field of condition monitoring, with a special focus on industrial applications. It covers both theoretical and experimental approaches, as well as a range of monitoring conditioning techniques and new trends and challenges in the field. Topics of interest include, but are not limited to: vibration measurement and analysis; infrared thermography; oil analysis and tribology; acoustic emissions and ultrasonics; and motor current analysis. Books published in the series deal with root cause analysis, failure and degradation scenarios, proactive and predictive techniques, and many other aspects related to condition monitoring. Applications concern different industrial sectors: automotive engineering, power engineering, civil engineering, geoengineering, bioengineering, etc. The series publishes monographs, edited books, and selected conference proceedings, as well as textbooks for advanced students.

** Indexing: Indexed by SCOPUS, WTI Frankfurt eG, SCImago

More information about this series at http://www.springer.com/series/13418

Ahmed Hammami · Philippus Stephanus Heyns ·
Stephan Schmidt · Fakher Chaari ·
Mohamed Slim Abbes · Mohamed Haddar
Editors

Modelling and Simulation of Complex Systems for Sustainable Energy Efficiency

Contributions to the First International Workshop on Modelling and Simulation of Complex Systems for Sustainable Energy Efficiency, MOSCOSSEE'2021, February 25–26, 2021

Springer

Editors
Ahmed Hammami
National School of Engineers of Gabes
Gabes, Tunisia

Philippus Stephanus Heyns
Centre for Asset Integrity Management,
Department of Mechanical
and Aeronautical Engineering
University of Pretoria
Pretoria, South Africa

Stephan Schmidt
Centre for Asset Integrity Management,
Department of Mechanical
and Aeronautical Engineering
University of Pretoria
Pretoria, South Africa

Fakher Chaari
National School of Engineers of Sfax
Sfax, Tunisia

Mohamed Slim Abbes
National School of Engineers of Sfax
Sfax, Tunisia

Mohamed Haddar
National School of Engineers of Sfax
Sfax, Tunisia

ISSN 2363-698X ISSN 2363-6998 (electronic)
Applied Condition Monitoring
ISBN 978-3-030-85583-3 ISBN 978-3-030-85584-0 (eBook)
https://doi.org/10.1007/978-3-030-85584-0

This Springer imprint is published by the registered company Springer Nature Switzerland AG
The registered company address is: Gewerbestrasse 11, 6330 Cham, Switzerland

Preface

The first “International Workshop on MOdelling and Simulation of COmplex Systems for Sustainable Energy Efficiency” MOSCOSSEE’2021 was organized by the LAboratory of Mechanics, Modelling and Production (LA2MP) from University of Sfax, Tunisia, and the Department of Mechanical and Aeronautical Engineering at the University of Pretoria, on 25 and 26 February 2021. This workshop is in the framework of a Tunisian South-African research project entitled “Design, Modelling and Diagnostic of Wind Turbines for Sustainable Energy Efficiency.” It was scheduled online due to the COVID-19 pandemic. The MOSCOSSEE’2021 workshop comprised high-level contributions in the fields of complex systems for sustainable energy efficiency in order to promote communication and collaboration between participants. Three plenary sessions were presented by eminent scientists who kindly agreed to share their knowledge in the workshop field. The organizers of the conference were honored by their participation with very interesting keynotes, namely

– Prof. José ANTUNES, Applied Dynamics Laboratory (ADL), Superior Technical Institute Lisbon, Portugal.
– Prof. Abdelkhalek ELHAMI, Mechanical Engineering Department, National Institute of Applied Sciences in Rouen (INSA de Rouen), France.
– Prof. Mohamed Amine BEN SOUF, National School of Engineers of Sfax, Tunisia.

This book contains 24 chapters selected from the presented papers by eminent scientists which were rigorously peer reviewed. During the 2 days of the workshop, oral communications discussed several topics such as

– Sustainable energy efficiency,
– Vibrations of complex systems,
– Structural and machine dynamics,
– Fault diagnosis and prognosis,
– Nonlinear dynamics,
– Vibration field measurements,

- Material behavior in dynamics,
- etc.

The editors are grateful to all participants from Tunisia, South Africa, Poland, Portugal and France, as well as the reviewers of the chapters. We acknowledge the financial support of the Ministry of Higher Education and Scientific Research in Tunisia and the National Research Foundation in South Africa under the Tunisia South Africa Agreement for Cooperation in Science and Technology. We would also like to thank Springer for their support of the MOSCOSSEE'2021 workshop.

February 2021

Ahmed Hammami
Philippus Stephanus Heyns
Stephan Schmidt
Fakher Chaari
Mohamed Slim Abbes
Mohamed Haddar

Contents

Numerical Assessment of the Structural Performance of a Segmented Wind Turbine Blade

Majdi Yangui(✉), Salma Thabti, Slim Bouaziz, and Mohamed Haddar

Mechanics, Modelling and Production Laboratory (LA2MP), Mechanic Department, National School of Engineers of Sfax, University of Sfax, BP 1173, 3038 Sfax, Tunisia
mohamed.haddar@enis.rnu.tn

Abstract. Segmented wind turbine blade (SWTB) development remains a major challenge for constructors so as to reduce blade transport and manufacturing costs. The blade structural properties must be examined in the design stage to enhance their mechanical behavior and fatigue life. This paper presents a numerical investigation of a SWTB prototype. Teeth inserted in holes at the interfaces of segments, were designed to avoid relative displacements between the segments assembled along a spar. Modal and fatigue analysis were established using ANSYS Workbench software to evaluate the structural performance of the investigated wind turbine blade (WTB). This work covers the impact of the assembly force and the rotation velocity effect on the blade fatigue life. Previous findings of an experimental study, of the SWTB at rest, were considered to validate the blade finite element model. To assess the used spar location, along the blade segments, the edgewise and flapwise deflections of the blade under assembly force effects were analysed. This study reveals the significant impact of the exerted assembly force on the SWTB fatigue life versus the rotation velocity effects. Interestingly, the obtained results indicate that a segments assembly force must be respected in the blade assembling to ensure the optimum service life.

Keywords: Fatigue analysis · Modal analysis · Segmented wind turbine blade · Finite element modeling

1 Introduction

In recent years, the concerns about the global warming consequences, caused essentially by the excessive fossil energy production, has made renewable energy development more and more indispensable for a sustainable future. In this context, wind energy is treated as one of the most profitable clean energy sources. Actually, power generation efficiency and cost represent the primary factors which govern wind turbine development. Thus, maintenance and manufacturing cost reduction remains a primary need. Undoubtedly, the wind turbine blades are the most crucial parts, in terms of performance and cost, of the wind power system. For this reason, many works have analysed the rotor blades fatigue and vibration, aiming to extend their service life. Shokrieh and Rafiee (2006) studied

A. Hammami et al. (Eds.): MOSCOSSEE 2021, ACM 20, pp. 1–7, 2022.
https://doi.org/10.1007/978-3-030-85584-0_1

the fatigue phenomena of a 23 m wind turbine blade (WTB) manufactured by the Vestas Company to predict its lifetime. By adopting a stochastic approach, the service life of the selected blade has been predicted to be limited to 18.66 years. Jensen et al. (2006) tested to failure, a composite WTB, under flapwise loading. The structure displacements were registered throughout the loading history. The experimental measurements and the numerical simulation results were processed to determine the location of the initial failure.

Recently, because of the intricacy of manufacturing and transport processes of the long WTBs, the blade fragmentation was proposed to solve such issues (Abdulaziz et al. 2018). Yangui et al. (2020) developed a numerical model of a SWTB using shell elements. To update the used material properties in the numerical model from the natural frequencies identified experimentally, an iterative technique was followed based on the substructuring technique. Dutton et al. (2001) tested a segmented form of a 13.4 m blade with a connecting tube to investigate the durability of the advanced fragmentation method. Static load tests, in the edgewise and flapwise directions were performed and repeated after a five million cycle fatigue test in the flapwise direction. The blade inspection shows that no damage was occurring in the segment interfaces and connections. Static and fatigue analysis of a SWBT were performed by Bhat et al. (2015) to evaluate its structural performance. The determined numerical results, of the non-segmented and the segmented blade, indicate that the effect of the fragmentation on the entire structural performance is minimal. Nevertheless, the outcomes of the load applied to assemble the segments were neglected. Yangui et al. (2019) performed an experimental analysis to inspect the effects of the assembly force adjusted by a nut on the WTB dynamical behavior. The determined experimental results, using the Eigen-system Realization Algorithm (ERA) modal identification method, showed the notable influence of the assembly force change on the blade eigenfrequencies versus the effects resulting from the blade rotation. Nevertheless, the impacts of the applied force on the blade shape and lifetime were not addressed.

In the present paper, an attempt to address this issue has been made by investigating the displacements and the fatigue life of a SWTB taking into account the mounting force of the segments. Based on previous experimental modal identification, the blade numerical model developed using Ansys Workbench software was validated. Static and fatigue analysis were performed to assess the effects resulting from the assembly force and the rotation velocity on the SWTB structural performance.

2 Blade Finite Element Modeling

A SWTB model, consisting of 5 segments assembled along a spar, was designed as seen in Fig. 1.

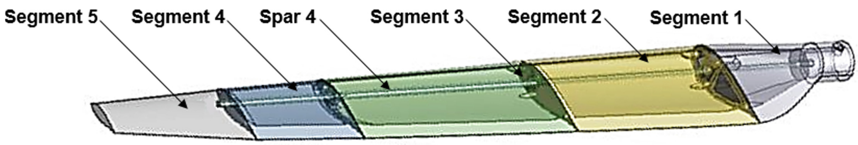

Fig. 1. Segmented blade CAD model

The full length of the designed blade is 500 mm and the segment skin thickness is about 3 mm. Regarding to the assembly, a spar with a length of 420 mm and a diameter of 4 mm was used. The material properties of the SWTB components are presented in the following Table 1.

Table 1. Material properties of the blade components.

Parameters	Material	Density (kg/m^3)	Poisson's ratio	Elastic modulus (GPa)
Blade segments	PC-ABS	1070	0.3879	2.25
Spar	Steel	7850	0.3	210

Using ANSYS Workbench finite element software, solid elements with three degrees of freedom per node and a free mesh were adopted to model the blade structure. Considering the blade segment's complex shape, the tetrahedral finite element was used. For the spar, the mesh was simplified by adopting the quadratic element as shown in Fig. 2.

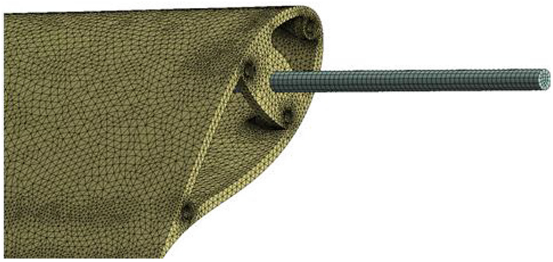

Fig. 2. Segmented blade mesh

To simulate the contact between the different parts of the blade, a frictional contact was defined between the segments and the spar and at the interfaces of segments. The contact between the tip and the root segments of the blade and the spar was bonded.

To validate the established numerical model, modal analysis was carried out without applying the assembly force. The assembled blade structure was clamped at its root. To optimise the mesh size, a convergence study was conducted for various mesh sizes. Accordingly, 979306 nodes and 613326 elements were generated. The natural frequencies, obtained numerically and those reached experimentally by Yangui et al. (2019), are given in Table 2.

Table 2. Segmented blade natural frequencies.

	Present work	Yangui et al. (2019)	Error %
1st natural frequency	17.9	17.4	2.87
2nd natural frequency	23.5	24.8	5.24
3rd natural frequency	80.9	85.7	5.60

An acceptable agreement is found, between the simulated and experimental findings, where the maximum error is about 5.6%. Thus, the introduced numerical model can be reliably employed to evaluate the fragmented blade structural performance.

3 Structural Performance Assessment

The WTB efficiency depends essentially on the blade shape. Thus, the segments mounting force and the spar location must be primarily treated during the blade design to avoid structural distortion. Figure 3 shows the blade tip edgewise and flapwise displacements for different assembly loads. In this section, only the static assembly load of the blade segments was exerted.

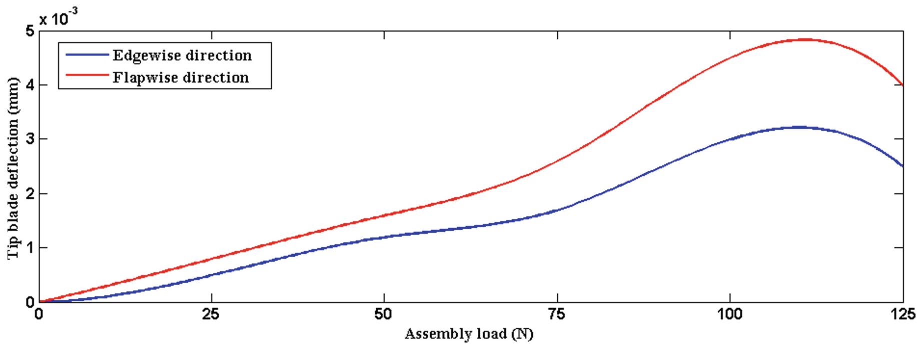

Fig. 3. Edgewise and flapwise displacements as a function of the assembly load.

The displacement amplitudes proved the negligible influence of the assembly force on the blade shape, where, up to a significant assembly effort of 125 N, the maximum deflection does not exceed 0.005 mm. Therefore, the spar location along the blade is well designed.

To assess the impact of the assembly force on the lifetime of the WTB structure, fatigue analysis was performed using Ansys Workbench fatigue module. Stress life type analysis was adopted based on Stress-Cycle (S-N) curves of the segments and spar materials. A bending load, in the flapwise direction, equal to 5 N was applied on the third blade segment as illustrated in Fig. 4. Based on the results obtained from the static load analysis, the fatigue analysis was performed where the zero-based constant amplitude loading type was assumed.

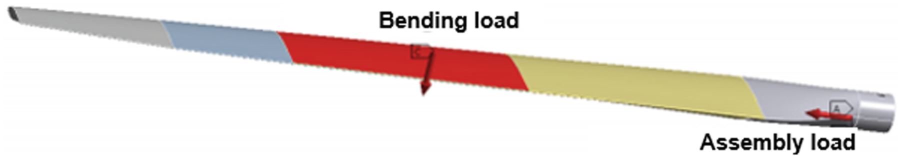

Fig. 4. Blade bending and assembly loads.

Figure 5 represents the SWTB lifetime change as a function of the applied assembly load.

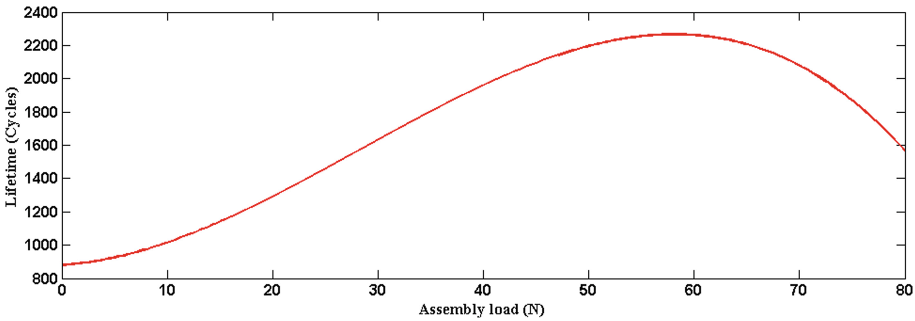

Fig. 5. Segments assembly load impact on the blade fatigue life.

It is observed that the lifetime of the blade is significantly dependent on the assembly load. The maximum fatigue life of the blades, equal to 2273 cycles, is obtained by applying an assembly load equal to 59 N. For an assembly load higher than 60 N, the blade cycles of fatigue life start to decrease.

To analyse the rotation velocity results on the blade fatigue life, a constant assembly load equal to 59 N was applied. The rotational velocity direction was performed as seen in Fig. 6.

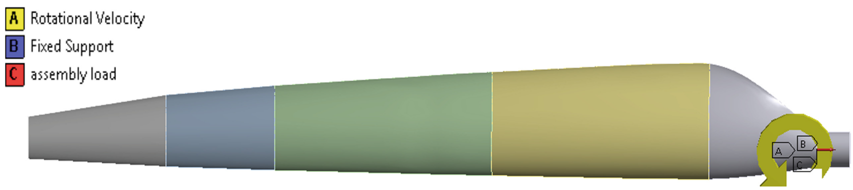

Fig. 6. Rotating blade model

Based on a static analysis, the blade fatigue life investigation was performed assuming a ratio loading type with a tolerance of 10%. Thus, the alternating load, provoked by the blade spinning velocity, was limited to 10% of the static load amplitude. The prediction of the rotating blade fatigue life is presented in Fig. 7.

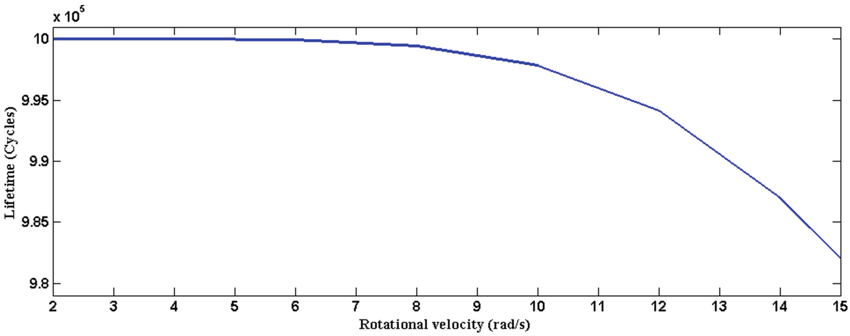

Fig. 7. Rotation velocity effects on the blade fatigue life.

Clearly, the increase of the WTB rotation velocity from 2 rad/s to 15 rad/s engenders a negligible loss of the blade fatigue life. Thus, the spar is well localized along blade segments in a way that it did not generate an important bending force component in the centrifugal load produced by the blade rotation.

4 Conclusion

In the present study, numerical analysis were performed to evaluate the structural performance of a SWTB. The numerical model of the blade was validated by reference to experimental analysis. The blade deflections, at rest, under the assembly load were determined the prove the satisfactorily location of the spar along the blade segments. Static and fatigue analysis were also performed to inspect the impacts of the segments assembly force and the rotation velocity on the blade fatigue life. Findings show that an assembly load must be respected during the WTB mounting to ensure the maximum service life, and thus, the sustainability of the wind turbine system. Again, the designed spar location was perfectly assessed by the negligible effects of the rotation velocity on the blade lifetime. In this work, only the flapwise bending fatigue was treated. Therefore, this research can be extended through the development of a dual-axis, edgewise and flapwise, fatigue testing.

References

Abdulaziz, A.H., Elsabbagh, A., Elnady, T.: Testing and validation of a novel segmented wind turbine blade. J. Test. Eval. **47**(5), 3719–3739 (2018)

Bhat, C., Noronha, D.J., Saldanha, F.A.: Structural performance evaluation of modularized wind turbine blade through finite element simulation. J. Energy Econ. Dev. **1**(1), 79 (2015)

Dutton, A.G., Kildegaard, C., Dobbe, T.: Design, structural testing, and cost effectiveness of sectional wind turbine blades. Technical Report JOR3970167 (2001)
Jensen, F.M., Falzon, B.G., Ankersen, J., Stang, H.: Structural testing and numerical simulation of a 34 m composite wind turbine blade. Compos. Struct. **76**(1–2), 52–61 (2006)
Shokrieh, M.M., Rafiee, R.: Simulation of fatigue failure in a full composite wind turbine blade. Compos. Struct. **74**(3), 332–342 (2006)
Yangui, M., Bouaziz, S., Taktak, M., Debut, V., Antunes, J., Haddar, M.: Numerical and experimental analysis of a segmented wind turbine blade under assembling load effects. J. Theor. Appl. Mech. **57**(1), 85–97 (2019)
Yangui, M., Bouaziz, S., Taktak, M., Haddar, M.: Experimental updating of a segmented wind turbine blade numerical model using the substructure method. J. Strain Anal. Eng. Des. **56**(2), 67–75 (2020)

Identifiability Considerations for Rotating Machine Fault Diagnosis and Prognosis

Stephan Schmidt(✉), P. Stephan Heyns, and Daniel N. Wilke

Centre for Asset Integrity Management, Department of Mechanical and Aeronautical Engineering, University of Pretoria, Pretoria, South Africa
stephan.schmidt@up.ac.za

Abstract. It is important to develop reliable fault diagnosis and prognosis methods for critical mechanical assets such as wind turbines. Reliable fault diagnosis and prognosis methods ensure that the damage is detected early, the damage modes are accurately characterised, and the correct remaining life is inferred. This enables the appropriate maintenance decisions to be made and can decrease the risk of unexpected breakdowns. Identifiability is an important criterion for the development of new fault diagnosis and prognosis methods. Therefore, in this work, we present the identifiability problem for fault diagnosis and prognosis on academic examples and we place a specific emphasis on gearbox applications. This chapter provides an overview of the concepts and is intended for neophytes to experienced researchers and practitioners. Hence, the examples are purposefully simple. We specifically highlight the importance of sensor positioning and also discuss the influence of varying operating conditions on the diagnosis and prognosis steps. Thereafter, we present the fundamental steps in the fault diagnosis and prognosis process and highlight the associated challenges with identifiability. We also propose potential solutions for these challenges. Lastly, we propose requirements for the different phases of the fault diagnosis and prognosis steps, which could be beneficial when developing new methods.

Keywords: Gearbox · Diagnosis · Prognosis · Identifiability · Bearing · Gears · Signal processing

1 Introduction

Condition-Based Maintenance (CBM), which comprises diagnosis and prognosis tasks, is important for expensive machine assets such as wind turbines [1]. Wind turbines, for example, are prone to gearbox, brake and rotor blade failures that result in long downtimes [1]. In CBM, condition monitoring data such as temperature, vibration, and pressure measurements are acquired from the machine and subsequently used to infer the health of the machine (i.e. diagnosis) and to determine the remaining useful life of the machine (i.e. prognosis) [1]. Vibration-based methods are most commonly used to monitor the condition of rotating machine components such as bearings and gears [2,3]

A. Hammami et al. (Eds.): MOSCOSSEE 2021, ACM 20, pp. 8–20, 2022.
https://doi.org/10.1007/978-3-030-85584-0_2

Usually, the damaged assets result in subtle changes in the condition monitoring data that are difficult to detect [2]. This makes processing the data into more meaningful representations essential. Several signal processing and learning-based[1] condition monitoring methods have been developed (e.g. Ref [4,5]) to address the challenges posed by the weak signal components-of-interest. Here, extraneous signal components, time-varying operating conditions, and non-Gaussian noise mask the components-of-interest and impede diagnosis [3,6].

Ultimately, the diagnosis and prognosis steps are used to inform maintenance decisions and therefore the diagnosis and prognosis methods should be carefully designed. In the diagnosis step, the damaged component and damage severity are inferred from the condition monitoring data and used for prognosis algorithms to predict the remaining useful life. Many data-driven prognosis approaches are proposed in the literature [7]. However, the methods require representative historical fault data from the different damage modes, which are difficult to obtain in practice [8]. Hence, inferring the relevant fault information is critical.

Therefore, in this work, we highlight that identifiability is essential for developing fault diagnosis and prognosis methods. Firstly, we present the identifiability problem for rotating machine condition monitoring in Sect. 2, whereafter we highlight the different tasks in the fault diagnosis and prognosis process in Sect. 3. In Sect. 4, we propose requirements for the development of fault diagnosis and prognosis methods, whereafter we conclude the work in Sect. 5.

2 Identifiability for Condition Monitoring

2.1 The Condition Monitoring Problem

Figure 1(a) shows the condition monitoring problem for a gearbox with four bearings (B1, B2, B3, B4), a gear, a pinion and two events E1 and E2. In Fig. 1(b), the sources of the events are shown: The pinion is damaged, resulting in event E1, and the outer race of the bearing is damaged, resulting in event E2. In this example, two sensors are placed on the casing of the gearbox S1 and S2. Ultimately, we would like to infer the gearbox's condition from one (or both) sensor(s) measurements. In this example, actual measurements from different sensors on a gearbox are shown to emphasise the influence of the sensor positions.

The excitations due to the damage should travel between the source (i.e. the events) and the sensors [9], with possible transmission paths highlighted in Fig. 1(c). The time domain signals can be decomposed as follows:

$$x_1(t) = h_{11}(t) \otimes e_1(t) + h_{12}(t) \otimes e_2(t) + n_1(t), \tag{1}$$

$$x_2(t) = h_{21}(t) \otimes e_1(t) + h_{22}(t) \otimes e_2(t) + n_2(t), \tag{2}$$

[1] We refer to statistical learning, machine learning and deep learning methods as learning-based methods.

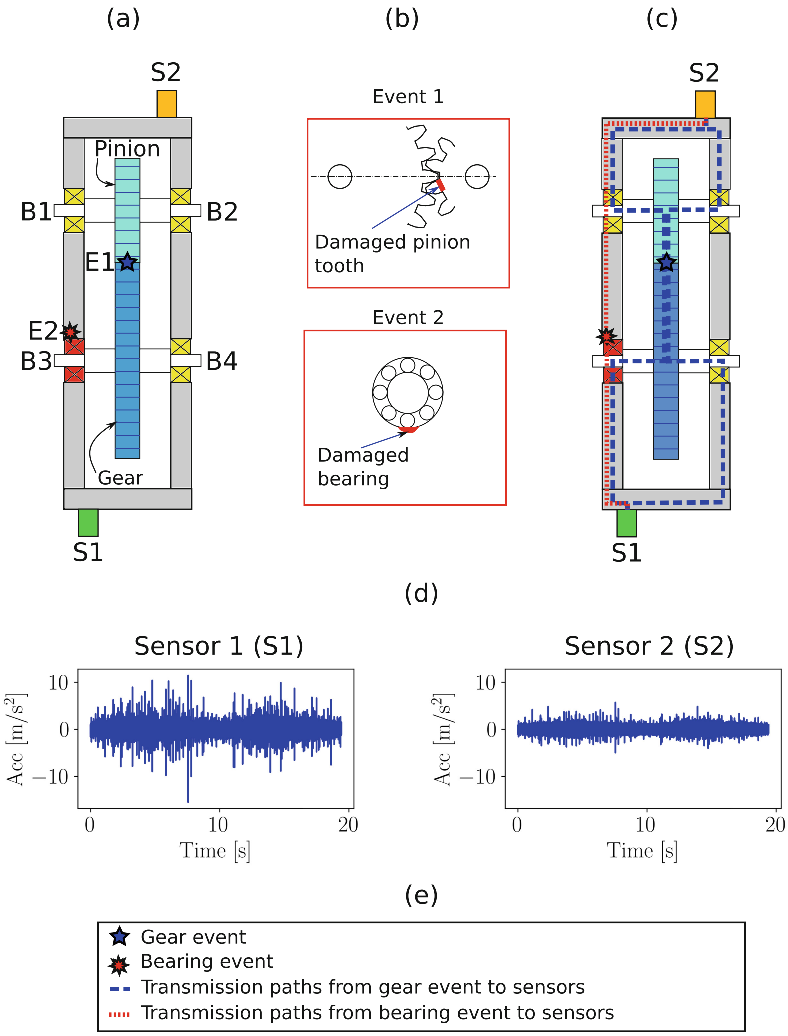

Fig. 1. The condition monitoring problem: (a) The gearbox, two events inside the gearbox E1 and E2, four bearings B1, B2, B3, B4 and two sensors, S1 and S2, are shown. (b) The two damage components causing the events are shown. (c) Some of the transmission paths between the events and the sensors are shown. (d) Example signals are shown for the two sensors. These were acquired from two sensors on the test-rig described in Ref. [3]. (e) The legend for the events and the transmission paths.

where $x_i(t)$ and $n_i(t)$ are the vibration signal and the extraneous components[2] in the ith sensor signal, respectively. The jth event, attributed to the excitation at the source of the damage (e.g. the rolling element's interaction with a spall), is denoted e_j. The impulse response function that captures the transmission path between event j and sensor i is denoted by h_{ij}. The measured vibration signal is discrete and denoted $\boldsymbol{x} = [x(0), x(\Delta t), x(2 \cdot \Delta t), \ldots]$, where Δt is the sampling period. By using the convolution theorem, it is possible to decompose the signals as follows:

$$\begin{bmatrix} X_1(f) \\ X_2(f) \end{bmatrix} = \begin{bmatrix} H_{11}(f) & H_{12}(f) \\ H_{21}(f) & H_{22}(f) \end{bmatrix} \begin{bmatrix} E_1(f) \\ E_2(f) \end{bmatrix} + \begin{bmatrix} N_1(f) \\ N_2(f) \end{bmatrix}, \tag{3}$$

where H_{ij}, X_i, E_j, N_i are the Fourier transforms of h_{ij}, x_i, e_j and n_i respectively. Changes in the signal X_i can potentially be influenced by changes in the frequency response function H_{i1} and H_{i2}; the events E_1 and E_2; and/or the noise components N_i. Therefore, it is important to carefully interpret the changes in the raw signal and its statistics. Ultimately, we desire to extract or enhance the event information E_j to perform diagnosis and prognosis.

2.2 Identifiability Problem

Identifiability and observability are closely related; observability indicates whether we can infer the latent state of the system from the system's response, while identifiability indicates whether we can infer the system's parameters from its response [10]. In condition monitoring, we typically would like to infer the parameters of the damage (e.g. size of the damage) and therefore we present this discussion in an identifiability context. We will use Eq. (3) to present the identifiability problem for condition monitoring, without accounting for estimation errors (e.g. the influence of finite length signals). We can write Eq. (3) in matrix form

$$\boldsymbol{X}(f) = \boldsymbol{H}(f) \cdot \boldsymbol{E}(f) + \boldsymbol{N}(f), \tag{4}$$

and leverage elementary linear algebra theory to gain insight into the identifiability of the events. The following four interesting cases are considered here for highlighting the identifiability problem:

$$\boldsymbol{H}_1 = \begin{bmatrix} a & 0 \\ 0 & b \end{bmatrix}, \quad \boldsymbol{H}_2 = \begin{bmatrix} a & c \\ c & b \end{bmatrix}, \quad \boldsymbol{H}_3 = \begin{bmatrix} a & a \\ a & a \end{bmatrix}, \quad \boldsymbol{H}_4 = \begin{bmatrix} a & 0 \\ 0 & 0 \end{bmatrix}. \tag{5}$$

where $a \in \mathbb{C}$, $b \in \mathbb{C}$, $c \in \mathbb{C}$. If the frequency response function matrix $\boldsymbol{H} = \boldsymbol{H}_1$, the events will feature independently in the sensors. Therefore, different sensors can be used to characterise specific events. If $\boldsymbol{H} = \boldsymbol{H}_2$ and assuming $\det(\boldsymbol{H}) \neq 0$, the matrix is invertible and therefore we obtain two signals with independent event information using

$$\boldsymbol{H}^{-1}(f) \cdot \boldsymbol{X}(f) = \boldsymbol{E}(f) + \boldsymbol{H}^{-1}(f) \cdot \boldsymbol{N}(f), \tag{6}$$

[2] Extraneous components refer to signal components attributed to physical mechanisms (e.g. healthy gear mesh components), environmental conditions and noise that are not related to the fault components-of-interest.

where $\boldsymbol{H}^{-1}(f) \cdot \boldsymbol{X}(f)$ is the spectrum of the processed signal. Note, that unless we know $\boldsymbol{N}(f)$, we cannot identify the events E_j, but only scaled and translated versions of the events, i.e. $\alpha \cdot E_j + \beta$. This is often sufficient for most condition monitoring tasks. If $\boldsymbol{H} = \boldsymbol{H}_3$, the rows are linearly dependent, which means that the sensors contain duplicate information (e.g. the sensors are symmetric for the structure and the excitations) and $\boldsymbol{H}_3$ is not invertible. This means that we cannot recover the original events from the response. Lastly, if $\boldsymbol{H} = \boldsymbol{H}_4$, it is only possible to identify the information concerning event 1; event 2 is not identifiable irrespective of the signal processing algorithm used. These four academic examples highlight the importance of sensor positioning to obtain well-conditioned matrices.

Many condition monitoring algorithms (e.g. [2,3,11]) only utilise the information from a single sensor to infer the machine's condition. In some classes of condition monitoring algorithms (e.g. [12,13]), we aim to design filters $P_{ij}(f)$ that can be applied to the data of a single sensor $X_j(f)$ so that the jth event is identifiable from the processed signals. The spectrum of these processed signals can be decomposed as follows:

$$\begin{bmatrix} P_{i1}(f) \\ P_{i2}(f) \end{bmatrix} X_i(f) = \begin{bmatrix} \alpha_1 & 0 \\ 0 & \alpha_2 \end{bmatrix} \cdot \begin{bmatrix} E_1(f) \\ E_2(f) \end{bmatrix} + \begin{bmatrix} \beta_1 \\ \beta_2 \end{bmatrix}, \tag{7}$$

where $P_{ij}(f) \cdot X_i(f)$ is the spectrum of the processed signal aiming to extract event E_j, α_i is a scaling term and β_i is an offset term. The scaled events E_j are identifiable if we can design a filter

$$P_{ij}(f) = k \cdot H_{ij}(f), \tag{8}$$

where $k \neq 0$ and $H_{i1}(f) \cdot H_{i2}(f) = 0$, i.e. the frequency response functions of the two events are independent. This is possible if the two events manifest in two separate narrow frequency bands. Targeted informative frequency band identification methods (e.g. [11,12]) and targeted blind deconvolution algorithms [13] aim to find the optimal filters $P_{ij}(f)$ to extract the events-of-interest.

In conclusion, the measurement signal (and its processed signal) is influenced by the [9]:

– transmission path, which means that it is influenced by the sensor location and the damaged component's location. Planetary gearboxes have time-varying transmission paths between the planet gears and the sensors [14].
– excitation characteristics (e.g. if there is a bearing crack or a bearing spall in the inner race or outer race).
– the extraneous components (e.g. dominant healthy gear mesh components, impulsive environmental noise).

All these effects can impede identifiability of the events and therefore impede the fault diagnosis and prognosis tasks discussed in the next section.

3 Fault Diagnosis and Prognosis

3.1 Overview of Diagnosis and Prognosis Steps

The diagnosis and prognosis problems are shown in Fig. 2 using the available information from a selected sensor. In the condition inference problem, we infer the actual condition (i.e. the damaged component, the damage mode and the size of the damage) from the processed condition monitoring data. The estimated condition is subsequently used with an appropriate degradation model (e.g. Paris' law) to estimate the system's remaining useful life. The reliability of the remaining useful life estimation process depends on our ability to diagnose the machine.

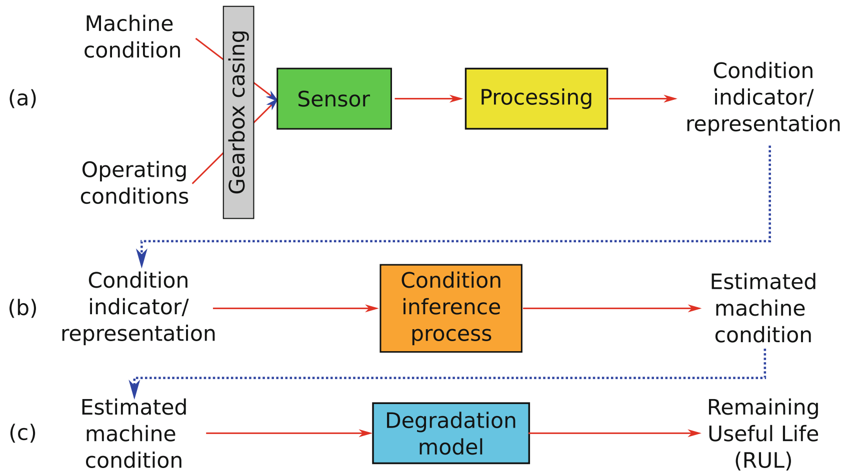

Fig. 2. The conventional diagnosis and prognosis problem. (a) Condition monitoring and data processing; (b) Diagnosis; (c) Prognosis.

In summary, the following steps need to be followed to perform diagnosis (Steps 1–4) and prognosis (Step 5):

1. Damage detection (Presented in Sect. 3.1)
2. Damage component identification (Presented in Sect. 3.2)
3. Damage mode identification (Presented in Sect. 3.3)
4. Fault severity quantification (Presented in Sect. 3.4)
5. Remaining useful life estimation (Presented in Sect. 3.5)

3.2 Damage Detection

In the damage detection phase, changes in the condition monitoring data due to the deteriorating machine are detected and flagged by comparing condition

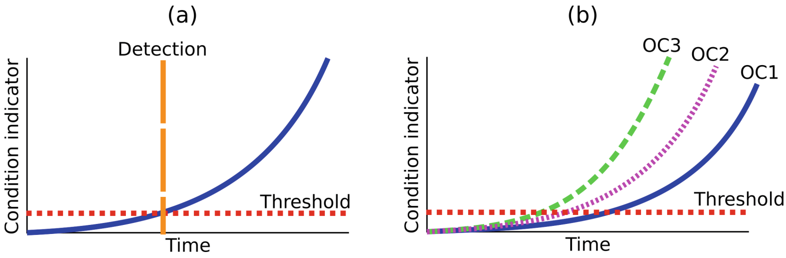

Fig. 3. (a) The generic fault detection problem is shown for a single threshold and fault detection point. (b) The influence of operating conditions on fault detection. Abbreviations: OC - Operating Condition.

indicators against thresholds as shown in Fig. 3(a). For example, the threshold can be determined using the statistical methodology proposed by Antoni and Borghesani [4]. In learning-based methods, the detection threshold is usually determined from the reference density obtained from healthy historical data [5]. However, time-varying operating conditions could influence the condition indicator and could therefore influence the time of detection (i.e. our ability to identify the damage) and increase the false positive rate (i.e. detecting changes due to operating condition as opposed to changes in machine condition). This is highlighted in Fig. 3(b). This problem can be alleviated by using the appropriate pre-processing of the signal (e.g. [15]) or post-processing of the condition indicators (e.g. [16]). For example, in Ref. [15], the amplitude modulation caused by the changes in the operating conditions is estimated and attenuated, while retaining the damage information. In contrast, Zimroz et al. [16] first obtain the relationship between a condition indicator and the wind turbine's power using a regression model . Thereafter, changes in this model are used for condition monitoring. It is expected that the sensitivity of the condition indicator to the operating conditions (e.g. power) is dependent on the condition of the machine and can therefore be used for damage detection.

3.3 Damage Component Identification

The damage component identification (also referred to as damage localisation) problem is shown in Fig. 4 for the example gearbox in Fig. 1. As shown in Fig. 4(a), the measured signal $\boldsymbol{x}$ can be generated by multiple potential events (e.g. a single damage mode or multiple simultaneous damage modes) and contains extraneous components $\boldsymbol{n} = [n(0), n(\Delta t), \ldots,]$. The damaged component is identifiable if we can process the signals $\boldsymbol{x}$ to extract the scaled events $\alpha \cdot e_i + \beta$. This is shown in Eq. (7) with the spectral representation. Methods to identify the damaged component include:

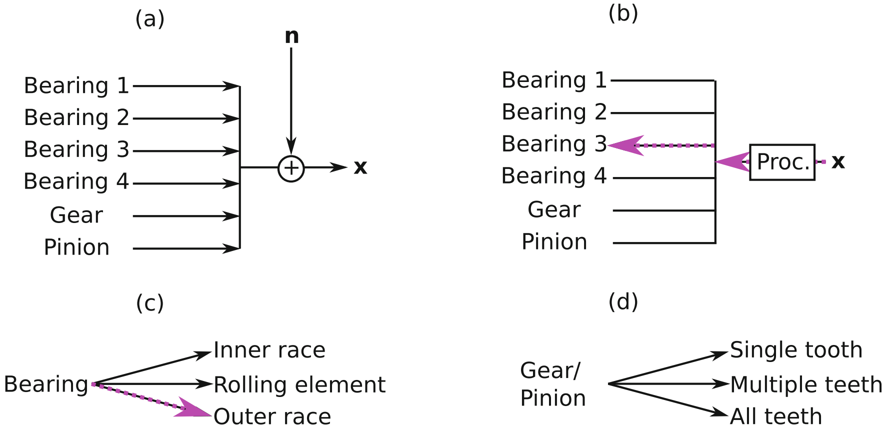

Fig. 4. The damage component identification problem: (a) The signal generation process for the gearbox in Fig. 1; (b) The damage subcomponent identification problem with bearing 3 identified using a Processing step; (c) Some of the potential bearing damage cases; (d) Some of the potential gear damage cases.

- The synchronous average can be used to extract synchronous deterministic components. If there are extraneous synchronous components, these components would contaminate the synchronous average and impede the damaged component's identifiability.
- The synchronous average of the squared envelope does not facilitate identifiability as it is sensitive to non-synchronous changes in the signal [3]. The synchronous median of the squared envelope and the synchronous geometric average of the squared envelope are much better suited as they are robust to non-synchronous impulsive components [3].
- Cyclostationary analysis tools such as the squared envelope spectrum, the spectral correlation and the improved envelope spectrum can be used to determine the characteristics of the component-of-interest [2]. Cyclostationary analysis methods for time-varying speed conditions are proposed in Refs. [17] and cyclostationary analysis methods for impulsive noise conditions are proposed in Ref. [6,18].
- In discrepancy analysis, the anomalies' localised behaviour is used to determine the source of the anomalous behaviour [19].
- In contrast to blind condition indicators, targeted condition indicators make it possible to focus on specific cyclic orders and can be used to target specific mechanical components [11]. The RMS for example is sensitive to any energy changes in the data and cannot be used to identify the damaged component and would therefore not be a reliable estimate of the fault severity.

To be able to perform damage identification, the rotational speed of a reference shaft and the system's kinematics (e.g. the gear mesh frequencies, the ball-pass outer race component of the bearing) need to be known [19]. The damaged component identifiability is also impeded if two components have the same statistical behaviour (e.g. both are first-order cyclostationary) and have very similar characteristic frequencies, e.g. if the same bearings are located on the same shaft. However, using multiple sensors might separate the contributions of the different sources if $\boldsymbol{H}$ in Eq. (4) is invertible.

3.4 Damage Mode Identification

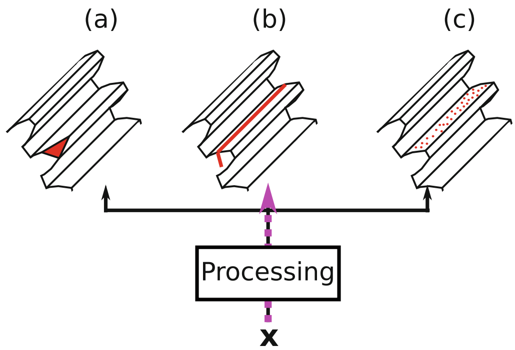

Fig. 5. The damage mode identifiability problem is illustrated when gear damage is present and only three damage modes are considered. The measured signal is processed to either identify (a) a tooth chip, (b) a tooth crack, or (c) pitting, with the tooth crack identified in this example.

In the damage mode identification phase, the mode of degradation (e.g. crack propagation in the gear tooth, pitting formation and spalling generation) is identified. The damage identification problem is shown in Fig. 5 for the case where there is gear damage in the gearbox. The degradation mode influences the remaining useful life of the system and therefore it is important to identify this for prognosis. Feng et al. [20] could distinguish between changes in the signals due to abrasive wear and pitting and therefore the damage mode is identifiable with their proposed procedure.

3.5 Fault Severity Quantification

In the fault severity quantification phase, the damage's size is estimated (e.g. characteristic crack length, material loss due to wear). This is important as the remaining useful life depends on the size of the damage [21] and this information needs to be known when using the appropriate degradation model. The ICS2 indicator, which measures the degree of second-order cyclostationarity, has a

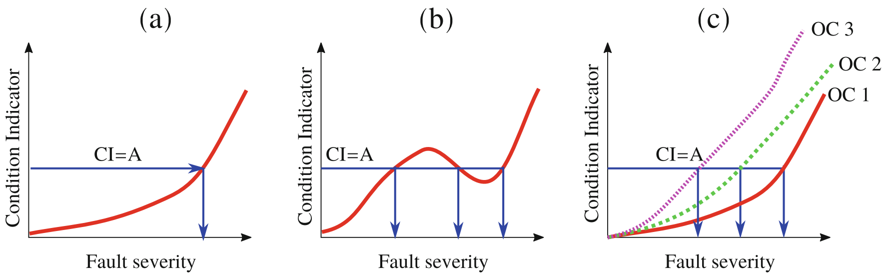

Fig. 6. The typical behaviour of condition indicators are shown. (a) The fault severity is identifiable for this specific case. (b) A condition indicator where the fault severity is not identifiable. (c) The fault severity is non-identifiable when a condition indicator is used that is sensitive to varying operating conditions. This behaviour is shown for three Operating Conditions (OC).

good correlation with the severity of the abrasive wear and pitting [20]. Three cases are shown in Fig. 6. These problems are often addressed in classification-based fault diagnosis, where the raw or processed data are mapped to a damage mode and/or a fault severity. The problem with this is that the degradation is continuous, not discrete, and often we do not have sufficient historical fault data to train the models [8]. Physics-based models can potentially aid with this task, but model calibration becomes an important consideration.

3.6 Remaining Useful Life (RUL) Estimation

The remaining useful life estimation process is shown in Fig. 7(a) for the ideal case and in Fig. 7(b) for the practical scenario. The larger the variance of the

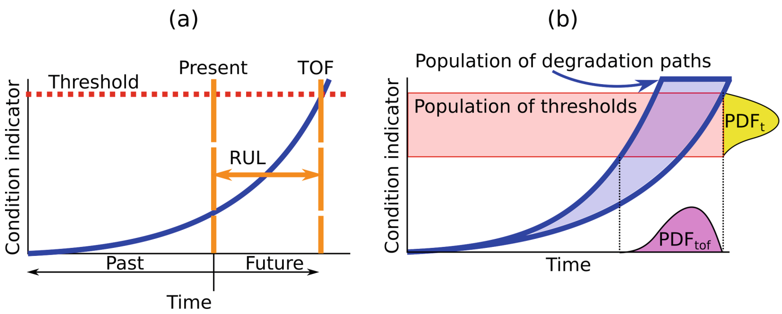

Fig. 7. The Remaining Useful Life (RUL) estimation process: (a) The conventional RUL estimation process is shown for a known threshold, a known degradation path and a known Time-Of-Failure (TOF). (b) The practical prognosis problem is illustrated as a population of failure thresholds, with the Probability Density Function (PDF) denoted by PDF_t, and a population of degradation paths. This makes us uncertain of the actual TOF, which is described by $\mathrm{PDF}_{\mathrm{tof}}$.